

First-principles study of edge chemical modifications in graphene nanodots

Huaixiu Zheng* and Walter Duley

Department of Physics and Astronomy, University of Waterloo, 200 University Avenue West, Waterloo, Ontario N2L 3G1, Canada

(Received 25 March 2008; revised manuscript received 22 May 2008; published 21 July 2008)

Rectangular graphene nanodots have both armchair and zigzag edges, which can be terminated with a variety of atoms or molecular groups. Our first-principles study shows that edge chemical modification can alter the electronic structure of graphene nanodots significantly. We find that when saturated with different atoms or molecular groups (such as -H, -F, -OH, etc.) on the zigzag edges, the graphene nanodots show a spin-polarized ground state, but with magnetic moment, spin density and energy gap are strongly dependent on the type of saturating atom or molecular group. Our results indicate that graphene nanodots have great potential to serve as future molecular sensor and transistor devices.

DOI: 10.1103/PhysRevB.78.045421

PACS number(s): 73.22.-f

I. INTRODUCTION

With experimental advances in the fabrication¹⁻⁵ of graphene materials, two-dimensional (2D) graphene, one-dimensional (1D) graphene nanoribbons (GNRs) and zero-dimensional (0D) graphene nanodots have been extensively studied from both experimental and theoretical points of view.⁶⁻¹³ The relativistic characteristics^{6,7} and outstanding electronic properties involving ballistic transport and large coherence length² make graphene an excellent platform for studying quantum electrodynamics (QED) phenomena.⁸ It is also a promising candidate material for future nanoelectronic^{3,9-11} and nanospintronic^{12,13} applications. What is more exciting is the very recent report of the successful fabrication of graphene quantum dots as small as 20 nm, with which a purely graphene-based single-electron transistor was realized and studied.¹⁴

Two particular types of GNRs with armchair and zigzag shaped edges have been extensively studied.¹⁵⁻¹⁹ In the tight-binding approximation, armchair graphene nanoribbons (A-GNRs) are predicted to be metallic when $n=3m+2$, where n is the width and m is an integer, and are insulating otherwise,^{11,15-21} while first-principles studies have shown that all A-GNRs have opened gaps with the introduction of edge deformations.¹¹ Zigzag graphene nanoribbons (Z-GNRs) are semiconducting with nonzero energy gaps due to the existence of ferromagnetically ordered edge states at each zigzag edge and an antiferromagnetic arrangement of spins between two zigzag edges.^{11,12} The application of an external electrical field across the ribbon can drive Z-GNRs into a half-metallic state where metallic electrons with one spin orientation coexist with insulating electrons having the other spin orientation.^{12,22}

Following the investigations of quasi-one-dimensional graphene nanoribbons, much research work has focused on the electronic and magnetic properties of quasi-zero-dimensional graphene nanodots.²²⁻²⁷ Due to the existence of both armchair and zigzag edges, finite 0D graphene nanodots also adopt spin-polarized edge states similar to 1D zigzag graphene nanoribbons. The half-metallic nature of 1D zigzag graphene nanoribbons under an external transverse electrical field is predicted to be preserved for 0D graphene nanodots.²⁴ However, quantum confinement and finite-size

effects greatly influence the electronic and magnetic properties of graphene nanodots as calculated with density functional theory (DFT).²³⁻²⁵

In a recent first-principles study,²⁴ it was shown that the spin density of graphene nanodots is localized on the two zigzag edges, which are terminated with hydrogen atoms. Due to the relative high spin density at the zigzag edges, the electronic structure of graphene nanodots could be very sensitive to terminations on the zigzag edges. Chemical modification of the edges is shown to induce metal-to-insulator transition and energy-gap variations²⁸ of armchair graphene nanoribbons and to alter low-bias transport²⁹ as well as to enhance the half-metallicity¹³ of zigzag graphene nanoribbons.

In this paper, we report the results of a first-principles study of the chemical modification effect. We find that the magnetic moment, spin density, highest occupied molecular orbital (HOMO) and lowest unoccupied molecular orbital (LUMO) state characteristics and the energy gap between the HOMO and LUMO states of finite graphene nanodots are strongly dependent on the choice of saturating atoms or molecular groups on the zigzag edges. Each different termination is found to tune the electronic structure uniquely. The terminations studied include hydrogen, fluorine, and oxygen atoms as well as hydroxyl and methyl functional groups as illustrated in Fig. 1. Following previous convention,²⁴ a $N \times M$ finite graphene nanodot is defined according to the number of dangling bonds on the armchair edges (N) and the number of dangling bonds on the zigzag edges (M). All the DFT calculations in this work were implemented with the GAUSSIAN suite of programs.³⁰ We have used the hybrid exchange-correlation functionals due to Becke, Lee, Yang, and Parr (B3LYP),³¹ which was shown to give a good representation of the characteristics of electronic structure in nanoscale and especially C-based systems.^{22,32,33} We have adopted the 3-21 G basis set,³⁴ which we find to be adequate when considering both computational efficiency and the accuracy of results.²³ For example, the energy gap for a 12×3 graphene nanodot is 1.491 eV obtained with the 3-21 G basis set compared to 1.504 eV from a 6-31 G basis set, while the computational time is doubled for the latter.

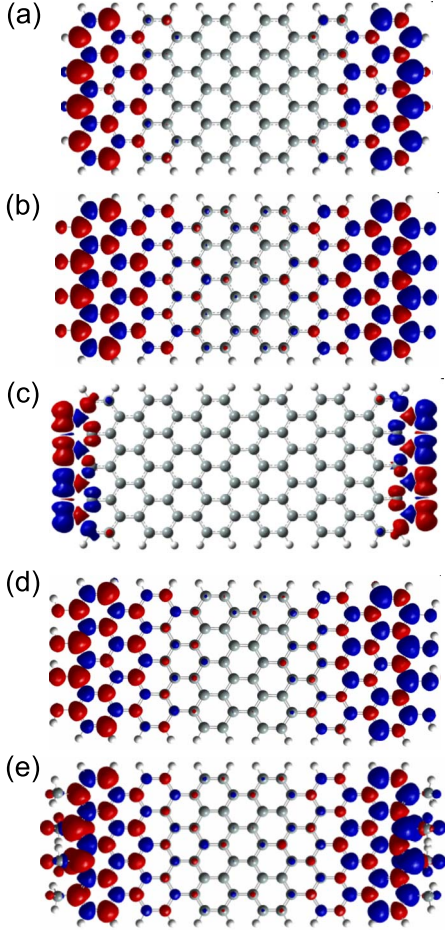


FIG. 1. (Color online) Isosurface spin densities (difference between α -spin and β -spin density) of the ground state of 12×4 graphene nanodots with different edge atoms or molecular groups at the zigzag edges: (a) -H, (b) -F, (c) -O, (d) -OH, and (e) -CH₃. Red: α spin; blue: β spin. The isovalue is 0.001.

II. SPIN DENSITY AND MAGNETIC MOMENT

All the geometrical structures reported here are fully relaxed by minimizing the total energy at the B3LYP level of theory without any other specific constraints. The initial bond length between all carbon atoms is set to 1.42 Å (which is the bond length of two-dimensional graphene) and the resulting geometrical structures are planar except the hydrogen atoms in hydroxyl and methyl functional groups. The optimized C-C bond lengths are between 1.36 Å and 1.46 Å, with the central bonds longer than the edge ones. The C-H bond on the armchair edges is approximately 1.08 Å in length. The optimized parameters for the bonds on the zigzag edges are listed in Table I, where d_{CX} represents the distance between edge carbon atom and the saturating atoms X (O, C for the hydroxyl and methyl cases, respectively).

Our spin unrestricted calculations show that the graphene nanodots present a spin-polarized singlet ground state with different terminal atoms or molecular groups on the zigzag edges. This is consistent with previous studies of magnetic ordering in finite graphene clusters.^{22–24,27} For 12×4

TABLE I. Length of bonds (d_{CX}) between edge carbon atoms and terminal atoms and difference of system energy between spin-polarized singlet state ($E_{\uparrow\downarrow}$) and triplet state ($E_{\uparrow\uparrow}$), spin-unpolarized singlet state (E_0) of 12×4 graphene nanodots with various terminations (X).

X	d_{CX} (Å)	$E_{\uparrow\downarrow} - E_{\uparrow\uparrow}$ (eV)	$E_{\uparrow\downarrow} - E_0$ (eV)
H	1.08	-0.0022	-0.77
F	1.36	-0.0020	-0.74
O	1.29	-0.3985	-0.90
OH	1.35 ~ 1.41	-0.0008	-0.60
CH ₃	1.52	-0.1724	-0.86

graphene nanodots, we have compared the following spin states: spin-polarized (open shell) singlet state, spin-polarized triplet state and spin-unpolarized (close shell) singlet state, whose total energies are $E_{\uparrow\downarrow}$, $E_{\uparrow\uparrow}$ and E_0 , respectively. The energetic ordering is $E_{\uparrow\downarrow} < E_{\uparrow\uparrow} < E_0$ for 12×4 graphene nanodots with the terminations (-H, -F, -O, -OH, -CH₃). The energy differences between $E_{\uparrow\downarrow}$ and $E_{\uparrow\uparrow}$, E_0 are shown in Table I. Note the sign of the energy difference is always negative, which means the spin-polarized singlet state has lower energy than both the triplet and spin-unpolarized singlet states. Thus, we conclude that the ground state remains a spin-polarized singlet state even when the zigzag edges are saturated with different atoms or molecular groups. In addition, it is also noticeable that the energies between spin-polarized singlet and triplet states of hydroxyl-group terminated system are very similar, which makes the magnetic ordering easy to be detected. Meanwhile, a close look also reveals that the fluorine-terminated system has the comparable stability (comparable energy difference between $E_{\uparrow\downarrow}$ and $E_{\uparrow\uparrow}$) to the hydrogen-terminated configuration, while oxygen- and methyl-terminated systems are more stable than hydrogen-terminated systems.

Furthermore, spin-density maps of the ground state show several other characteristics as shown in Fig. 1. First of all, while the spin arrangement on adjacent atoms is antiferromagnetic (AF) in the four cases: -H, -F, -OH, and -CH₃, in the ketonated system a mixed configuration of magnetic ordering appears on the zigzag edges. Both up- and down-spin waves appear on the same zigzag edge as shown in Fig. 1(c). On each zigzag edge, the up-spin wave is only sustained for half of the edge and the down-spin wave dominates the other half. This is quite different from the result for the 1D graphene nanoribbon ketonated system, where the magnetic ordering is antiferromagnetic on both edges.¹³ This difference is attributed to a finite-size effect that makes a less strong effective spin correlation. Second, the presence of different terminations significantly changes the spin densities of the carbon atoms on the zigzag edges, as can be seen qualitatively in Fig. 1. Quantitatively, the largest local magnetic moments of carbon atoms (M_C) on zigzag edges and terminal atoms or groups (M_X) are given in Table II. For the methyl-terminated system, M_C is larger and M_X smaller compared to those in the hydrogenated system. Conversely, systems terminated by fluorine, oxygen, and hydroxyl have smaller M_C and larger M_X compared to the hydrogenated

TABLE II. The largest local magnetic moments of carbon atoms (M_C) and terminal atoms or groups (M_X) of 12×4 graphene nanodots with various terminations (X).

X	M_C (μ_B)	M_X (μ_B)
H	0.434537	0.018155
F	0.363568	0.039413
O	0.089167	0.487594
OH	0.309457	0.093818
CH ₃	0.470425	0.040428

system. These differences originate from charge transfer between edge carbon atoms and terminations induced by differences in electronegativity. For example, the fluorine atom is more electronegative than the hydrogen atom and thus attracts more charge (electron/spin) from the carbon atoms. As a result, fluorine atoms have larger magnetic moments than hydrogen atoms as shown in Table II. For the ketonated system, the p electrons in oxygen atoms strongly affect the magnetic arrangement on the edge and greatly weaken the antiferromagnetic ordering, leading to a mixed configuration. Correspondingly, the carbon atoms on the edges have a very small magnetic moment.

III. ENERGY GAP AND HIGHEST OCCUPIED MOLECULAR ORBITAL—LOWEST UNOCCUPIED MOLECULAR ORBITAL

Having studied the impact of chemical edge modifications on the spin density and magnetic ordering, we now turn to a discussion of the energy gap between HOMO and LUMO states as well as the orbital configurations corresponding to these states. It is well known that the HOMO and LUMO states in finite graphene nanodots are either localized at the edge or form delocalized extended states, depending on the size of the system.^{23,25} The calculated energy gap between HOMO and LUMO states for 12×4 graphene nanodots terminated with different atoms and molecular groups on the zigzag edges is shown in Fig. 2. Other studies have found that the band gap of zigzag graphene nanoribbons (1D counterparts of 0D graphene nanodots) is only slightly changed in oxidized systems compared to fully hydrogenated ribbons.¹³ The magnetic ordering on the edges of zigzag graphene nanoribbons of oxidized systems is also antiferromagnetic.¹³ However, quantum confinement and finite-size effects make the electronic structure of 0D graphene nanodots very sensitive to chemical edge modification. At the B3LYP level of theory, we find, for example, that when zigzag edges are terminated with methyl groups, the energy gap in 12×4 graphene nanodots increases to 1.707 eV compared to 1.668 eV in the hydrogenated system. When zigzag edges are terminated with fluorine, hydroxyl groups, and oxygen atoms, the HOMO-LUMO energy gap decreases to 1.60 eV, 1.228 eV, and 0.817 eV, respectively. This result demonstrates that the energy gap can be tuned significantly by chemical modification of zigzag edges with different atomic and molecular groups. This effect can be very large; for example, the

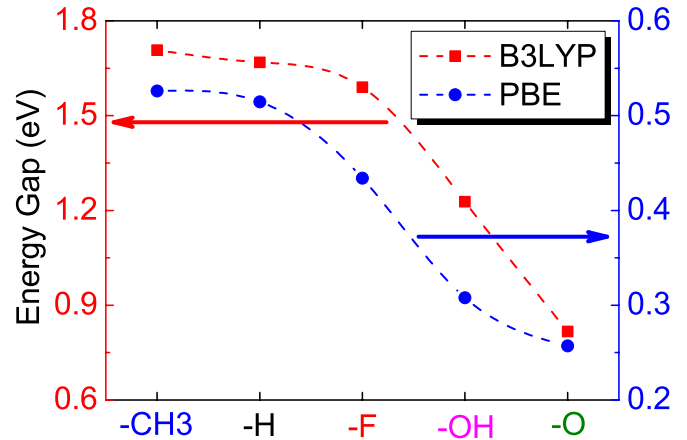


FIG. 2. (Color online) Energy gap between HOMO and LUMO for 12×4 graphene nanodots with zigzag edges terminated by -H, -F, -O, -OH, and -CH₃. Red squares represent the results obtained with B3LYP functional and blue dots represent those obtained with PBE functionals. Note that there is about a factor of 3 difference between the energy scale of B3LYP and PBE.

HOMO-LUMO gap decreases by roughly 50% when zigzag edges are oxidized. This is attributed to the participation of p electrons of oxygen atoms in the π electron system as noted above. To confirm our conclusion and show that the modification effect is independent of the exchange-correlation functional we chose, we also carried out the same energy-gap calculation with the semilocal gradient corrected functional of Perdew, Burke and Ernzerhof (PBE).^{35,36} As shown in Fig. 2, the PBE result exhibits similar energy-gap modulation behavior with B3LYP. Although the energy magnitude of PBE differs approximately by a factor of 3 with B3LYP, the general trend of gap variations we studied here is the same. To explore the origin of this significant gap modulation, we plot the density of states (DOS) of 12×4 graphene nanodots having different edge modifications in Fig. 3. The Fermi level is indicated by a vertical dashed line in each figure. A full width at half maximum (FWHM) of 0.2 was used to make the DOS peaks smooth. From Figs. 3(a)–3(c), we find that the profile of the density of states distribution for hydrogen, fluorine, and methyl terminated graphene nanodots are quite similar with only a slight shift in the Fermi level under effective potential induced by the attached atoms or functional groups. This occurs because hydrogen, fluorine, and the methyl group provide one extra electron to saturate the dangling σ electron of carbon atoms at the zigzag edge. As a result, the σ orbitals are removed from the vicinity of the Fermi level, with only the vertical-to-plane π orbital left in the vicinity of the Fermi level. However, after saturating the carbon σ electron, the hydroxyl group and an oxygen atom still have extra p electrons that can mix with the carbon π electron system. As a result, the DOS profile of hydroxyl and oxygen terminated graphene nanodots are quite different from hydrogen-terminated species with regard to both peak position and peak height [Figs. 3(c) and 3(d)]. In particular, one and two gap states appear in the vicinity of the Fermi level (as indicated by the arrows) for hydroxyl and oxygen terminations, respectively. Their appearance significantly alters the electronic structure near the Fermi level and narrows

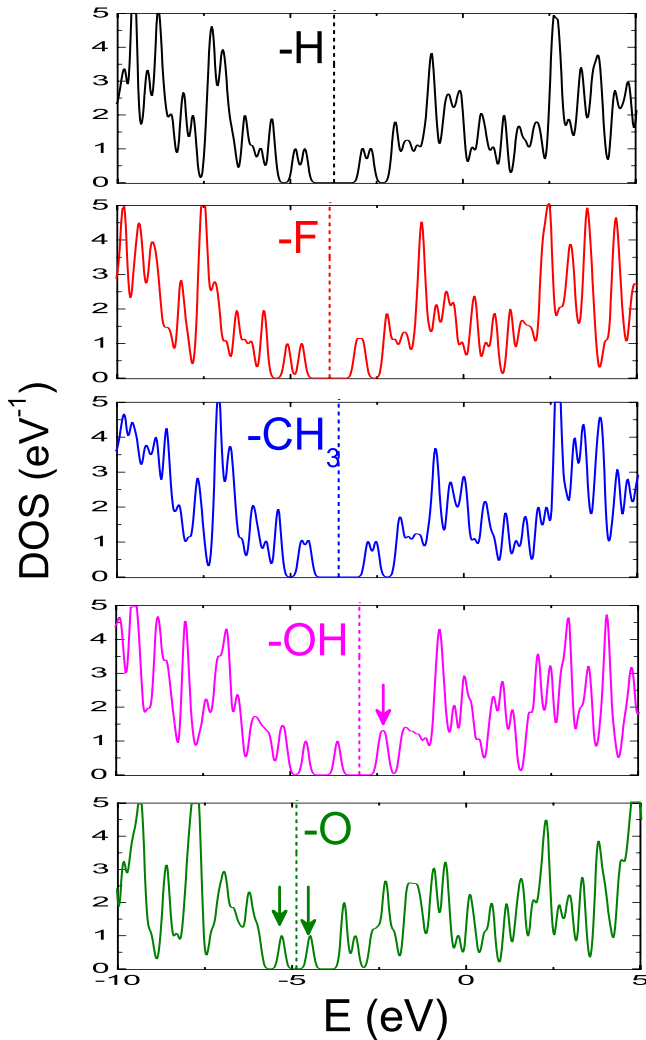


FIG. 3. (Color online) DOS for 12×4 graphene nanodots with zigzag edges terminated by -H, -F, -O, -OH, and $-\text{CH}_3$. The Fermi level is indicated by the vertical dashed line. The full width at half maximum is set to 0.2. The arrows indicate the modification-induced gap states.

the gap between HOMO and LUMO energy levels.

The effect of chemical modification on the orbital nature of HOMO and LUMO states is shown in Fig. 4. It is apparent that fully hydrogenated 12×4 graphene nanodots exhibit clear localization of HOMO and LUMO states confined to the zigzag edge regions. This is consistent with results from

a previous study of 0D graphene nanoribbons.²³ Similar edge localization of HOMO and LUMO states is also found in 12×4 systems terminated with fluorine atoms and methyl groups (not shown in Fig. 4). When the zigzag edges are saturated with oxygen atoms, the HOMO and LUMO states convert to delocalized extended states with the orbitals uniformly distributed along the graphene nanodots. The participation of p electrons of an oxygen atom in the π electron system causes the HOMO and LUMO states to change from an edge-localized configuration to an extended-delocalized distribution. However, a completely different configuration is observed for HOMO and LUMO states in hydroxyl-terminated systems. As shown in Fig. 4(c), the HOMO state is found to exhibit edge localization, while the LUMO state orbital is largely distributed at the center of the nanodot. It is also interesting that the orbital symmetry of the HOMO and LUMO orbitals is broken when the system is terminated with hydroxyl groups. This is attributed to a change of molecular point group from the high-symmetry C_{2v} group in the hydrogenated system to the low-symmetry configuration C_1 in the hydroxylated system.

IV. CONCLUSION

In conclusion, we have demonstrated that the chemical modification of zigzag edges can significantly alter the electronic and magnetic properties of graphene nanodots since a large proportion of the spin density is localized on the zigzag edges. The spin density, magnetic moment, as well as the HOMO-LUMO energy gap are highly dependent on the choice of terminating atoms or molecular groups on the zigzag edges and each atom or molecular group has a unique effect on these properties. In addition, it is also found that the HOMO and LUMO orbital configurations can be changed from an edge-localized to extended-delocalized distribution. Our results indicate that careful control of chemical termination in these structures could provide an opportunity to tailor 0D graphene nanodots for specific sensor applications as well as for applications in the field of spintronic devices. The delocalization of HOMO-LUMO states introduced by edge modifications could make the graphene nanodots insensitive to edge defects which are inevitable in experimental fabrication procedure of samples. This will provide more stable charge-spin transport behavior mediated by 0D graphene nanodots. Our results of energy-gap modulation also provide an alternative way to achieve graphene-based transistors in addition to field-effect transistors.

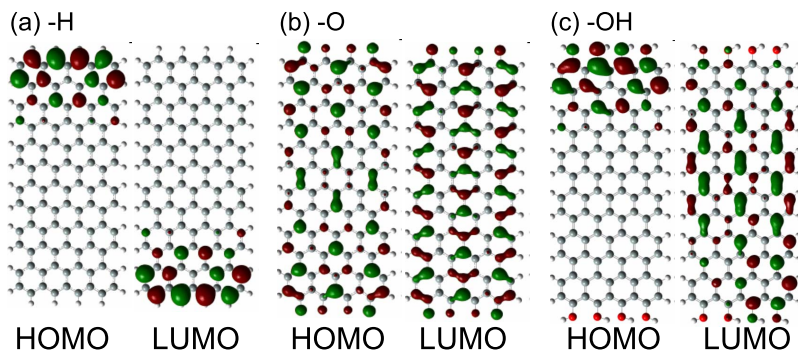


FIG. 4. (Color online) Isosurface molecular orbital map of the α -spin HOMO and LUMO with different terminal atoms or molecular groups on the zigzag edges: (a) -H, (b) -O, and (c) -OH. Color code: red, positive; green, negative. The isovalue is 0.02.

ACKNOWLEDGMENTS

This research was supported by a grant from the NSERC

of Canada. This work was made possible by the facilities of the Shared Hierarchical Academic Research Computing Network (SHARCNET: www.sharcnet.ca).

*Corresponding author; h27zheng@uwaterloo.ca

- ¹K. S. Novoselov, A. K. Geim, S. V. Morozov, D. Jiang, Y. Zhang, S. V. Dubonos, I. V. Grigorieva, and A. A. Firsov, *Science* **306**, 666 (2004).
- ²C. Berger, Z. Song, X. Li, X. Wu, N. Brown, C. Naud, D. Mayou, T. Li, J. Hass, A. N. Marchenkov, E. H. Conrad, P. N. First, and W. A. de Heer, *Science* **312**, 1191 (2006).
- ³M. Y. Han, B. Özyilmaz, Y. Zhang, and P. Kim, *Phys. Rev. Lett.* **98**, 206805 (2007).
- ⁴B. Özyilmaz, P. Jarillo-Herrero, D. Efetov, D. A. Abanin, L. S. Levitov, and P. Kim, *Phys. Rev. Lett.* **99**, 166804 (2007).
- ⁵A. L. Vazquez de Parga, F. Calleja, B. Borca, M. C. G. Passeggi, Jr., J. J. Hinarejos, F. Guinea, and R. Miranda, *Phys. Rev. Lett.* **100**, 056807 (2008).
- ⁶Y. Zhang, Y.-W. Tan, H. L. Stormer, and P. Kim, *Nature (London)* **438**, 201 (2005).
- ⁷K. S. Novoselov, Z. Jiang, Y. Zhang, S. V. Morozov, H. L. Stormer, U. Zeitler, J. C. Maan, G. S. Boebinger, P. Kim, and A. K. Geim, *Science* **315**, 1379 (2007).
- ⁸M. I. Katsnelson, K. S. Novoselov, and A. K. Geim, *Nat. Phys.* **2**, 620 (2006).
- ⁹B. Obradovic, R. Kotlyar, F. Heinz, P. Matagne, T. Rakshit, M. D. Giles, M. A. Stettler, and D. E. Nikonov, *Appl. Phys. Lett.* **88**, 142102 (2006).
- ¹⁰Y. Ouyang, Y. Yoon, J. K. Fodor, and J. Guo, *Appl. Phys. Lett.* **89**, 203107 (2006).
- ¹¹Y.-W. Son, M. L. Cohen, and S. G. Louie, *Phys. Rev. Lett.* **97**, 216803 (2006).
- ¹²Y.-W. Son, M. L. Cohen, and S. G. Louie, *Nature (London)* **444**, 347 (2006).
- ¹³O. Hod, V. Barone, J. E. Peralta, and G. E. Scuseria, *Nano Lett.* **7**, 2295 (2007).
- ¹⁴L. A. Ponomarenko, F. Schedin, M. I. Katsnelson, R. Yang, E. W. Hill, K. S. Novoselov, and A. K. Geim, *Science* **320**, 356 (2008).
- ¹⁵M. Fujita, K. Wakabayashi, K. Nakada, and K. Kusakabe, *J. Phys. Soc. Jpn.* **65**, 1920 (1996).
- ¹⁶K. Nakada, M. Fujita, G. Dresselhaus, and M. S. Dresselhaus, *Phys. Rev. B* **54**, 17954 (1996).
- ¹⁷K. Wakabayashi, M. Fujita, H. Ajiki, and M. Sigrist, *Phys. Rev. B* **59**, 8271 (1999).
- ¹⁸M. Ezawa, *Phys. Rev. B* **73**, 045432 (2006).
- ¹⁹L. Brey and H. A. Fertig, *Phys. Rev. B* **73**, 235411 (2006).
- ²⁰H. Zheng, Z. F. Wang, T. Luo, Q. W. Shi, and J. Chen, *Phys. Rev. B* **75**, 165414 (2007).
- ²¹K. Sasaki, S. Murakami, and R. Saito, *J. Phys. Soc. Jpn.* **75**, 074713 (2006).
- ²²E. Rudberg, P. Salek, and Y. Luo, *Nano Lett.* **7**, 2211 (2007).
- ²³P. Shemella, Y. Zhang, M. Mailman, P. M. Ajayan, and S. K. Nayak, *Appl. Phys. Lett.* **91**, 042101 (2007).
- ²⁴O. Hod, V. Barone, and G. E. Scuseria, *Phys. Rev. B* **77**, 035411 (2008).
- ²⁵O. Hod, J. E. Peralta, and G. E. Scuseria, *Phys. Rev. B* **76**, 233401 (2007).
- ²⁶P. G. Silvestrov and K. B. Efetov, *Phys. Rev. Lett.* **98**, 016802 (2007).
- ²⁷M. Ezawa, *Phys. Rev. B* **76**, 245415 (2007).
- ²⁸Z. F. Wang, Q. Li, H. Zheng, H. Ren, H. Su, Q. W. Shi, and J. Chen, *Phys. Rev. B* **75**, 113406 (2007).
- ²⁹D. Gunlycke, J. Li, J. W. Mintmire, and C. T. White, *Appl. Phys. Lett.* **91**, 112108 (2007).
- ³⁰M. J. Frisch *et al.*, GAUSSIAN 03, Revision C.02, Gaussian, Inc., Wallingford CT, 2004.
- ³¹A. D. Becke, *J. Chem. Phys.* **98**, 5648 (1993).
- ³²S. Yang and M. Kertesz, *J. Phys. Chem. A* **110**, 9771 (2006).
- ³³E.-J. Kan, Z. Li, J. Yang, and J. G. Hou, *Appl. Phys. Lett.* **91**, 243116 (2007).
- ³⁴K. D. Dobbs and W. J. Hehre, *J. Comput. Chem.* **8**, 880 (1987).
- ³⁵J. P. Perdew, K. Burke, and M. Ernzerhof, *Phys. Rev. Lett.* **77**, 3865 (1996).
- ³⁶J. P. Perdew, K. Burke, and M. Ernzerhof, *Phys. Rev. Lett.* **78**, 1396 (1997).